Journal of Solid State Chemistry **155,** 62–70 (2000)
doi:10.1006/jssc.2000.8892, available online at http://www.idealibrary.com on IDEAL®

Layered Cobalt Phosphates by the Amine Phosphate Route

Amitava Choudhury,*,† Srinivasan Natarajan,* and C. N. R. Rao*,†,[1]

*Chemistry and Physics of Materials Unit, Jawaharlal Nehru Centre for Advanced Scientific Research, Jakkur P.O., Bangalore 560 064, India; and †Solid State and Structural Chemistry Unit, Indian Institute of Science, Bangalore 560 012, India

Received May 30, 2000; in revised form July 18, 2000; accepted July 27, 2000

DEDICATED TO PROFESSOR J. M. HONIG

Two layered cobalt phosphates, I, $[NH_3CH_2CH(OH)CH_2NH_3][Co_2(PO_4)_2]$, and II, $[NH_3CH_2CH(OH)CH_2NH_3][Co_2(HPO_4)_3]$, have been hydrothermally synthesized employing the reaction of 1,3-diammonium-2-hydroxy propane with Co^{II} ions. While in I, the layers are made of 3- and 4-membered rings, they are made by 4- and 12-membered rings in II. The layers are held together by strong hydrogen bond interactions between the amine and the framework. I contains Co–O–Co linkages and becomes ferrimagnetic around 30 K, unlike II with only Co–O–P linkages which is paramagnetic. Crystal data are as follows: I, orthorhombic, $a = 22.894(2)$, $b = 7.568(1)$, $c = 6.697(1)$ Å, $V = 1160.3(2)$ Å^3, space group = *Pbcn* (no. 60), $Z = 8$, $M = 399.87$, $D_{calc.} = 2.287$ gcm^{-3}, $\mu(MoK\alpha) = 3.176$ mm^{-1}, $\lambda = 0.71073$ Å, $R_1 = 0.06$, $S = 1.27$; II, monoclinic, $a = 8.608(3)$, $b = 9.640(3)$, $c = 17.258(2)$ Å, $\beta = 93.23(1)^\circ$, $V = 1429.9(2)$ Å^3, space group = $P2_1/c$ (no. 14), $Z = 4$, $M = 497.94$, $D_{calc.} = 2.313$ gcm^{-3}, $\mu(MoK\alpha) = 2.729$ mm^{-1}, $\lambda = 0.71073$ Å, $R_1 = 0.03$, $S = 1.05$. © 2000 Academic Press

INTRODUCTION

Amongst the open-framework metal phosphates, those of transition metals are small in number (1). While several iron phosphates have been characterized (2–5), very few cobalt phosphates are reported in the literature (6). The known cobalt phosphates, by and large, possess three-dimensional architectures. Thus, Stucky and co-workers have characterized several cobalt phosphates possessing zeolite-like structures (7, 8). To our knowledge, only two cobalt phosphate structures with layered architecture have been synthesized in the presence of organic amines (9). It has been shown recently that the reaction of metal ions with amine phosphates provides a facile route for the synthesis of open-framework metal phosphates (10, 11). By employing this method, we recently prepared three-dimensional cobalt phosphates (12). In this report, we describe the synthesis of two layered cobalt phosphates by the reaction of 1,3-diammonium-2-hydroxy propane phosphate (DAHP-P) with Co(II) ions. The cobalt phosphates have the compositions, $[NH_3CH_2CH(OH)CH_2NH_3][Co_2(PO_4)_2]$, **I**, and $[NH_3CH_2CH(OH)CH_2NH_3][Co_2(HPO_4)_3]$, **II**.

EXPERIMENTAL

The amine phosphate, DAHP-P, was synthesized by the following procedure. An amount of 2.008 g of 1,2-diamino-2-hydroxy propane (DAHP) was dissolved in 2 ml of water, and 1.82 ml of H_3PO_4 (85 wt%) was added dropwise to the solution to result in white precipitate. A mixture of the composition, DAHP: $1.2H_3PO_4$:$5H_2O$, was sealed in a polypropylene bottle along with the precipitate and heated at 110°C for 6 h. The resulting product contained large quantities of needle-like crystals, which were filtered and washed with a minimum quantity of water. The crystals were stable in air and were characterized by single-crystal X-ray diffraction.

Compounds **I** and **II** were synthesized hydrothermally by reacting DAHP-P with Co^{2+} ions under nonaqueous conditions. Thus, for **I**, 0.357 g of $CoCl_2 \cdot 6H_2O$ was dispersed in 3 ml of THF, resulting in a clear blue solution. To this, 0.564 g of DAHP-P and 0.63 ml of triethylamine (TEA) were added under continuous stirring. The final mixture with a composition of $CoCl_2 . 6H_2O$:2DAHP-P:3TEA:25THF, was sealed in a PTFE-lined stainless-steel autoclave, and was heated at 180°C for 44 h. The resulting product, a crop of deep blue plate-like crystals, was vacuum filtered, washed with ethanol, and dried under ambient conditions. A synthesis mixture with the composition $CoCl_2 . 6H_2O$:2DAHP-P:28 butan-2-ol, heated at 180°C for 62 h, yielded blue rod-like crystals of **II**. While a basic pH (~8.5) was found to favor the formation of **I**, **II** was prepared under near acidic conditions (pH ~ 6). Compound **II** is rather unstable and undergoes hydrolysis, giving rise to a pink-colored product. The as-synthesized compounds are

[1]To whom correspondence should be addressed. E-mail: cnrrao@jncasr.ac.in.

0022-4596/00 $35.00

TABLE 1
X-Ray Powder Data for Compound I, $[NH_3CH_2(CH(OH)CH_2NH_3][Co_2(PO_4)_2]$

h	k	l	$2\theta_{obs}$	$\Delta(2\theta)^a$	d_{calc}	d_{obs}	$\Delta(d)^b$	$I_{rel}{}^c$
2	0	0	7.733	0.008	11.444	11.432	−0.012	100.0
4	0	0	15.493	0.008	5.722	5.719	−0.003	6.0
3	1	1	21.230	0.026	4.190	4.185	−0.005	16.5
5	1	0	22.707	0.000	3.916	3.916	0.000	1.0
6	0	0	23.328	0.010	3.815	3.813	−0.002	< 1
2	2	0	24.803	0.003	3.590	3.590	0.000	7.6
0	2	1	27.111	0.030	3.292	3.289	−0.003	1.8
4	2	0	28.285	−0.006	3.154	3.155	0.001	8.2
3	0	2	29.129	0.009	3.066	3.066	0.000	7.5
2	1	2	30.236	0.023	2.958	2.956	−0.002	2.6
6	2	0	33.359	−0.006	2.685	2.686	0.001	8.6
1	2	2	36.063	0.023	2.492	2.490	−0.002	4.7
7	0	2	38.460	−0.017	2.340	2.341	0.001	< 1
8	2	0	39.487	−0.011	2.281	2.282	0.001	3.5
8	1	2	43.297	0.019	2.090	2.090	0.000	1.6
9	0	2	44.738	−0.007	2.025	2.026	0.001	1.0
1	2	3	47.422	−0.035	1.916	1.917	0.001	1.2
4	4	0	50.860	−0.007	1.795	1.795	0.000	1.5
14	0	0	56.277	0.009	1.635	1.635	0.000	< 1
11	2	2	57.547	−0.017	1.601	1.602	0.001	1.7

[a] $2\theta_{obs} - 2\theta_{calc}$.
[b] $d_{obs} - d_{calc}$.
[c] $100 \times I/I_{max}$.

TABLE 3
Atomic Coordinates [$\times 10^4$] and Equivalent Isotropic Displacement Parameters [$Å^2 \times 10^3$] for the Amine Phosphate (DAHP-P), $[C_3N_2OH_{12}][HPO_4]$

Atom	x	y	z	U(eq)[a]
P(1)	2183(2)	4536(2)	6619(1)	26(1)
O(1)	2585(6)	4528(4)	5779(2)	39(1)
O(2)	−375(5)	4714(4)	6771(2)	29(1)
O(3)	3303(6)	2942(4)	7000(2)	43(1)
O(4)	3487(6)	6147(5)	6998(2)	68(1)
N(1)	7818(6)	−2050(5)	6878(2)	32(1)
N(2)	7096(6)	3432(4)	5471(2)	28(1)
C(1)	8412(8)	−1109(6)	6193(2)	31(1)
C(2)	7296(7)	649(6)	6150(2)	26(1)
C(3)	7970(8)	1624(6)	5452(2)	31(1)
O(10)	4826(5)	455(4)	6130(2)	35(1)

[a] U(eq) is defined as one-third of the trace of the orthogonalized U_{ij} tensor.

characterized using powder X-ray diffraction (XRD), thermogravimetric analysis (TGA), and elemental analysis by EDAX. A least-squares fit of the powder XRD lines (Cu$K\alpha$) lines, using the *hkl* indices garnered from single-crystal X-ray data, gave cell parameters that were in agreement

TABLE 2
Crystal Data and Structure Refinement Parameters for 1,3-DAHP-P, $[NH_3CH_2(CH(OH)CH_2NH_3][Co_2(PO_4)_2]$, and $[NH_3CH_2(CH(OH)CH_2NH_3][Co_2(HPO_4)_3]$, II

Structural Parameter	1,3-DAHP-P	I	II
Empirical formula	$P_1O_5C_3N_2H_{13}$	$Co_2P_2O_9C_3N_2H_{12}$	$Co_2P_3O_{13}C_3N_2H_{15}$
Crystal system	Monoclinic	Orthorhombic	Monoclinic
Space group	$P2_1/n$ (no. 14)	$Pbcn$ (no. 60)	$P2_1/c$ (no. 14)
a (Å)	5.721(2)	22.894(2)	8.608(3)
b (Å)	7.755(1)	7.568(1)	9.640(3)
c (Å)	17.537(2)	6.697(1)	17.258(2)
β (°)	94.7(1)	90.0	92.2(2)
Volume (Å^3)	775.5(2)	1160.3(2)	1429.9(2)
Z	4	8	4
Formula mass	188.12	399.87	497.9
ρ_{calc} (gcm^{-3})	1.611	2.287	2.313
μ(mm^{-1})	0.388	3.176	2.729
θ range (°)	2.33–23.30	1.78–23.28	2.26–23.26
Total data collected	3040	4389	5779
Index ranges	$-6 \le h \le 6$, $-4 \le k \le 8$, $-19 \le l \le 19$	$-25 \le h \le 14$, $-8 \le k \le 8$, $-7 \le l \le 7$	$-7 \le h \le 9$, $-10 \le k \le 10$, $-19 \le l \le 19$
Unique data	1117	839	2053
Data [$I > 2\sigma(I)$]	774	661	1730
Refinement method	Full-matrix least-squares on $\|F^2\|$	Full-matrix least-squares on $\|F^2\|$	Full-matrix least-squares on $\|F^2\|$
R_{int}	0.06	0.08	0.04
$R[I > 2\sigma(I)]$	$R_1 = 0.05$[a]; $wR_2 = 0.13$[b]	$R_1 = 0.06$[a]; $wR_2 = 0.16$[b]	$R_1 = 0.03$[a]; $wR_2 = 0.07$[b]
R (all data)	$R_1 = 0.08$; $wR_2 = 0.14$	$R_1 = 0.09$; $wR_2 = 0.19$	$R_1 = 0.04$; $wR_2 = 0.08$
Goodness of fit (S)	1.09	1.27	1.05
No. of variables	101	95	209
Largest difference map peak and hole eÅ^{-3}	0.361 and −0.412	1.187 and −1.328	0.902 and −0.562

[a] $R_1 = \sum||F_o| - |F_c||/\sum|F_o|$.
[b] $wR_2 = \{\sum[w(F_o^2 - F_c^2)^2]/\sum[w(F_o^2)^2]\}^{1/2}$. $W = 1/[\sigma^2(F_o)^2 + (aP)^2 + bP]$, $P = [\max(F_o^2, 0) + 2(F_c)^2]/3$, where $a = 0.0724$ and $b = 0.0$ for DAHP-P, $a = 0.1063$ and $b = 1.8798$ for **I**, $a = 0.0308$ and $b = 2.720$ for **II**.

with those determined by single-crystal XRD. The powder XRD data for **I** are presented in Table 1. Magnetic susceptibility measurements on **I** and **II** were carried out with a Lewis coil magnetometer in a field of 0.5 T.

A suitable single crystal of each compound was carefully selected under a polarizing microscope and glued to a thin glass fiber with cyanoacrylate (superglue) adhesive. Single-crystal structure determination by X-ray diffraction was performed on a Siemens Smart-CCD diffractometer equipped with a normal focus, 2.4-kW sealed tube X-ray source (Mo$K\alpha$ radiation, $\lambda = 0.71073$ Å) operating at 50 kV and 40 mA. A hemisphere of intensity data was collected using SMART software (13) at room temperature in 1321 frames with ω scans (width of 0.30° and exposure time of 20 s per frame) in the 2θ range 3° to 46.5°. The total collected data were reduced using the SAINT (13) program, and the orientation matrix along with the detector and the cell parameters were refined for every 40 frames on all the measured reflections. Pertinent experimental details for the structure determinations are presented in Table 1.

An empirical absorption correction based on symmetry equivalent reflections was applied using the SADABS (14) program. Other effects, such as absorption by glass fiber, were simultaneously corrected. The structures of **I** and **II** were solved by direct methods using SHELXS-86 (15), which readily established all the heavy atom positions (Co and P) and facilitated the identification of most of the other fragments (O, C, N, and H) from difference Fourier maps. All the hydrogen positions were initially located in the difference Fourier maps, and for the final refinement, the hydrogen atoms were placed geometrically and held in the riding mode. The last cycles of refinement included atomic positions for all the atoms, anisotropic thermal parameters for all the nonhydrogen atoms, and isotropic thermal parameters for all the hydrogen atoms. Full-matrix-least-squares structure refinement against $|F^2|$ was carried out using the SHELXTL-PLUS (16) package of programs. Details of the final refinements are given in Table 2. The final atomic coordinates for DAHP-P, **I**, and **II** are presented in Table 3, 4, and 6.

TABLE 4

Atomic Coordinates [$\times 10^4$] and Equivalent Isotropic Displacement Parameters [Å$^2 \times 10^3$] for I, [$NH_3CH_2(CH(OH)CH_2NH_3][Co_2(PO_4)_2$]

Atom	x	y	z	U(eq)[a]
Co(1)	2596(1)	112(2)	980(2)	21(1)
P(1)	1722(1)	2046(4)	3349(4)	19(1)
O(1)	2155(3)	407(9)	3491(9)	25(2)
O(2)	3196(3)	1853(9)	208(11)	28(2)
O(3)	3078(3)	− 1994(10)	1442(10)	30(2)
O(4)	1108(3)	1384(9)	3171(10)	28(2)
N(1)	1030(5)	− 2191(13)	3622(14)	45(3)
C(1)	510(8)	− 2967(25)	2907(56)	144(14)
C(2)	0000	− 2296(21)	2500	56(6)
O(10)	− 205(7)	− 2862(20)	4900(22)	43(7)

[a] U(eq) is defined as one-third of the trace of the orthogonalized U_{ij} tensor.

RESULTS AND DISCUSSION

The structure of the amine phosphate, DAHP-P [$C_3N_2OH_{12}$][HPO_4], is presented in Fig. 1. The structure

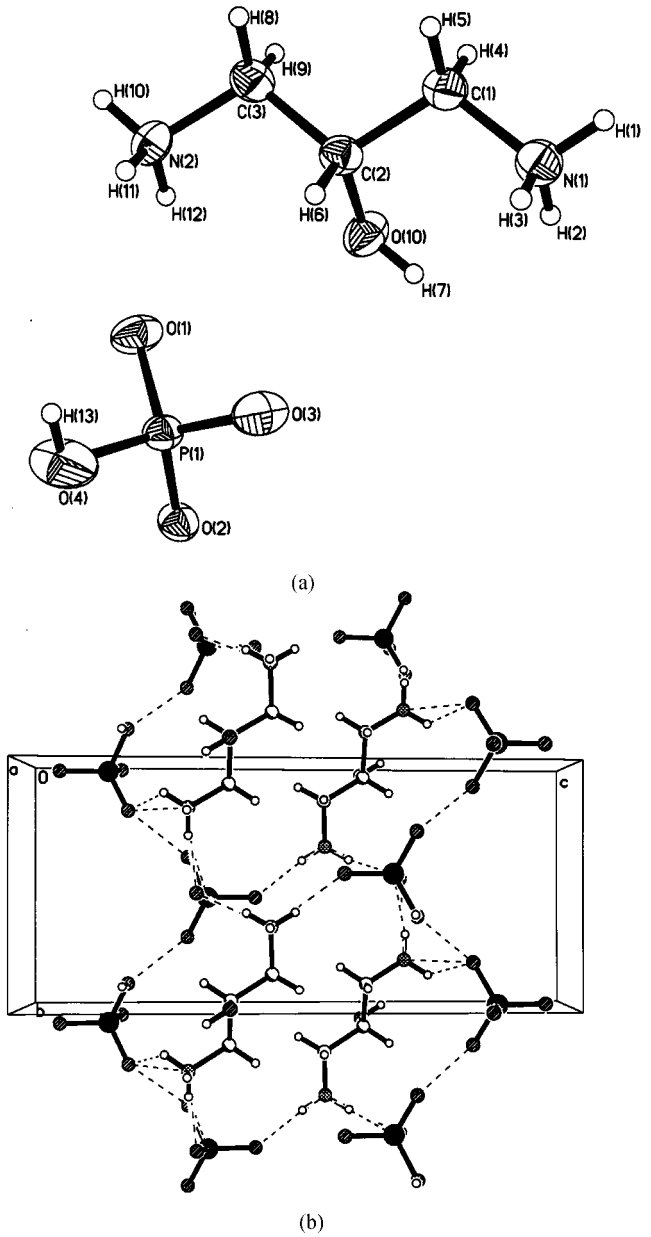

FIG. 1. (a) ORTEP plot of the amine phosphate, DAHP, [$C_3N_2OH_{12}$][HPO_4] showing the asymmetric unit. Thermal ellipsoids are given at 50% probability. (b) Packing drawing of the amine phosphate, DAHP, along the *ab* plane. Note that the noncovalent interactions between the hydrogen phosphate units form a cavity, wherein the amine molecules are present.

consists of a hydrogen-bonded network involving the HPO_4 tetrahedra and the diprotonated amine,DAHP. The individual moieties are arranged such that the HPO_4 and the DAHP unit alternate along the *ab* plane (Fig. 1b). Similar hydrogen-bonded structures of the amine phosphates have been described recently (17).

Both **I** and **II** are obtained by the hydrothermal reaction between the DAHP-P and Co^{II} ions. The structure of the compounds consist of a network of CoO_4 and PO_4 tetrahedra-forming layered architectures. The asymmetric unit of **I** contains 10 nonhydrogen atoms (Fig. 2a), of which 6 belong to the framework and 4 to the guest. The Co atom is tetrahedrally coordinated by oxygens with a cobalt oxygen distance $(Co-O)_{av}$ of 1.974 Å. Of the four oxygens that are connected with Co, three oxygens connect with the distinct P atom via Co–O–P linkage and the fourth oxygen links up with the adjacent Co atom forming infinite one-dimensional Co–O–Co linkages. The P atom makes three P–O–Co bonds and the remaining is a terminal P–O bond. The P–O

TABLE 5
Selected Bond Distances and Angles in I, $[NH_3CH_2(CH(OH)CH_2NH_3][Co_2(PO_4)_2]$

Moiety	Distance (Å)	Moiety	Distance (Å)
Co(1)–O(1)	1.974(7) [0.4666][a]	P(1)–O(1)	1.592(7) [1.0699]
Co(1)–O(1)^{i}	1.987(7) [0.4505]	P(1)–O(2)^{ii}	1.510(7) [1.3353]
Co(1)–O(2)	1.972(7) [0.4691]	P(1)–O(3)^{iii}	1.539(7) [1.2346]
Co(1)–O(3)	1.964(7) [0.4794]	P(1)–O(4)	1.497(7) [1.3830]
	Organic moiety		
N(1)–C(1)	1.41(2)	C(2)–O(10)	1.73(2)
C(1)–C(2)	1.30(2)	C(2)–O(10)^{vii}	1.73(2)
C(2)–C(1)^{vii}	1.30(2)		
Moiety	Angle (°)	Moiety	Angle (°)
O(3)–Co(1)–O(1)	104.2(3)	O(4)–P(1)–O(2)^{ii}	111.6(4)
O(2)–Co(1)–O(1)	120.3(3)	O(4)–P(1)–O(3)^{iii}	111.8(4)
O(3)–Co(1)–O(1)^{i}	104.9(3)	O(2)^{ii}–P(1)–O(3)^{iii}	112.8(4)
O(2)–Co(1)–O(1)^{i}	105.4(3)	O(4)–P(1)–O(1)	109.2(4)
O(1)–Co(1)–O(1)^{i}	118.5(4)	O(2)^{ii}–P(1)–O(1)	107.6(4)
O(3)–Co(1)–O(2)	101.1(3)	O(3)^{iii}–P(1)–O(1)	103.4(4)
P(1)–O(1)–Co(1)	110.8(4)	P(1)^{v}–O(2)–Co(1)	132.2(4)
P(1)–O(1)–Co(1)^{iv}	121.4(4)	P(1)–O(3)–Co(1)	132.9(4)
Co(1)–O(1)–Co(1)^{iv}	115.6(4)		
	Organic moiety		
C(2)–C(1)–N(1)	132(2)	C(1)–C(2)–O(10)	87(2)
C(1)^{vii}–C(2)–C(1)	134(2)	O(10)–C(2)–O(10)^{vii}	151(2)
C(1)–C(2)–O(10)^{vii}	82(2)		

Note. Symmetry transformations used to generate equivalent atoms: (i) $x, -y, z-\frac{1}{2}$; (ii) $-x+\frac{1}{2}, -y+\frac{1}{2}, z+\frac{1}{2}$; (iii) $-x+\frac{1}{2}, y+\frac{1}{2}, z$; (iv) $x, -y, z+\frac{1}{2}$; (v) $-x+\frac{1}{2}, -y+\frac{1}{2}, z-\frac{1}{2}$; (vi) $-x+\frac{1}{2}, y-\frac{1}{2}, z$; (vii) $-x, y, -z+\frac{1}{2}$.

[a] Bond valence values are given in brackets.

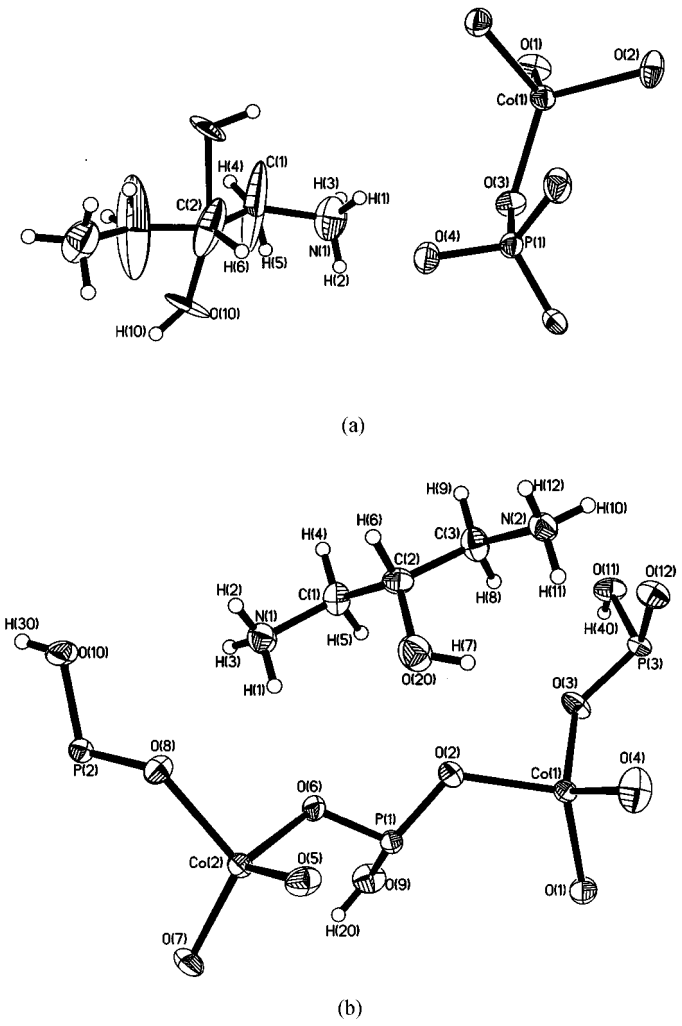

FIG. 2. (a) ORTEP plot of **I**, $[NH_3CH_2(CH(OH)CH_2NH_3][Co_2(PO_4)_2]$. Asymmetric unit is labeled. Thermal ellipsoids are given at 50% probability. (b) ORTEP plot of **II**, $[NH_3CH_2(CH(OH)CH_2NH_3][Co_2(HPO_4)_3]$.

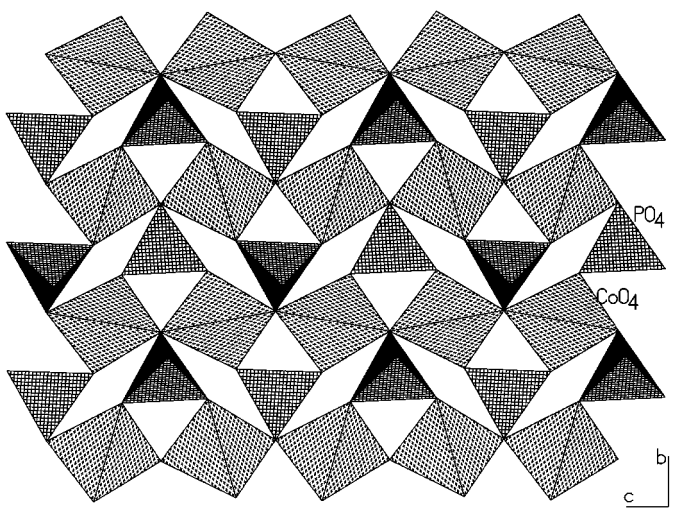

FIG. 3. Structure of **I**, $[NH_3CH_2(CH(OH)CH_2NH_3][Co_2(PO_4)_2]$, along the *bc* plane showing the layer arrangement. Note that connectivity gives rise to infinite Co–O–Co linkages.

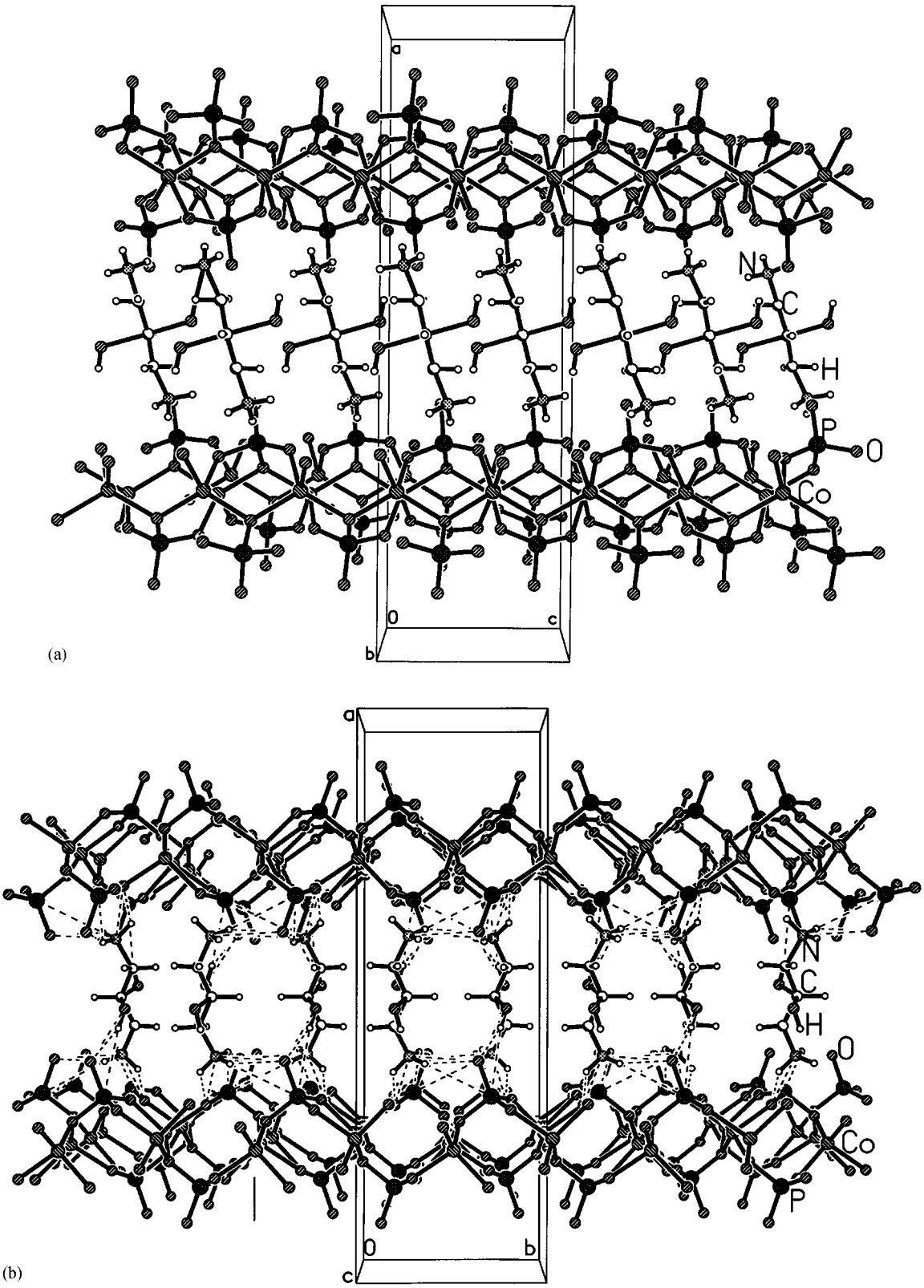

FIG. 4. (a) Structure of **I**, $[NH_3CH_2(CH(OH)CH_2NH_3][Co_2(PO_4)_2]$, along the *b* axis showing the layer arrangement. The hydrogen bond interactions between the amine molecule and the framework oxygens are not shown. (b) Structure of **I** along the *c* axis. Dotted lines represent hydrogen bond interactions. Note that the strongest interactions are between the P=O and the hydrogens of the amine.

TABLE 6
Atomic Coordinates [$\times 10^4$] and Equivalent Isotropic Displacement Parameters [$Å^2 \times 10^3$] for II, $[NH_3CH_2(CH(OH)CH_2NH_3][Co_2(HPO_4)_3]$

Atom	x	y	z	U(eq)[a]
Co(1)	3298(1)	1338(1)	9795(1)	15(1)
Co(2)	− 2394(1)	− 4817(1)	9795(1)	15(1)
P(1)	80(1)	2528(1)	10116(1)	15(1)
P(2)	− 5521(1)	4114(1)	8907(1)	15(1)
P(3)	4529(1)	− 1024(1)	8718(1)	15(1)
O(1)	3867(4)	1239(4)	10903(2)	26(1)
O(2)	1063(4)	1695(3)	9579(2)	26(1)
O(3)	3375(4)	− 484(3)	9283(2)	23(1)
O(4)	4528(4)	2799(4)	9383(2)	34(1)
O(5)	− 1011(4)	6314(3)	9486(2)	23(1)
O(6)	− 1383(3)	3018(3)	9666(2)	20(1)
O(7)	− 3290(4)	4848(3)	10813(2)	24(1)
O(8)	− 3918(3)	4784(3)	8897(2)	19(1)
O(9)	− 408(4)	1572(3)	10799(2)	28(1)
O(10)	− 5987(4)	3738(3)	8043(2)	25(1)
O(11)	3869(4)	− 2460(3)	8389(2)	25(1)
O(12)	4614(4)	− 109(3)	8005(2)	24(1)
N(1)	− 2719(4)	1768(4)	8227(2)	26(1)
C(1)	− 1446(5)	870(5)	7970(3)	25(1)
C(2)	− 194(5)	1735(5)	7617(3)	22(1)
O(20)	314(4)	2840(4)	8101(2)	33(1)
C(3)	1124(5)	809(5)	7396(3)	25(1)
N(2)	2384(4)	1654(4)	7081(2)	23(1)

[a] U(eq) is defined as one-third of the trace of the orthogonalized U_{ij} tensor.

distances are in the range 1.497(7)–1.592(7) Å, the longest distance being associated with the three-coordinated oxygen and the shorted being a P=O bond. Selected bond distances, bond valence parameters, and angles for **I** listed in Table 5 are in agreement with the literature values (6–9) for similar compounds.

The layered framework structure of **I** is built up from CoO_4 and PO_4 tetrahedra sharing vertices, forming 3- and 4-membered rings (Fig. 3). The connectivity between these building units forms a layered architecture. The terminal P=O group of the PO_4 unit project into the interlamellar space in an alternating pattern above and below the plane (Figs. 4a and 4b). Di-protonated 1,3-diamino-2-hydroxy propane molecules occupy the interlamellar space and interact with the framework via hydrogen bond interactions (Figs. 4a and 4b). Thus, in **I**, the inorganic and organic layers alternate. Similar layer arrangements are common in open-framework metal phosphates.

The asymmetric unit of **II** contains 23 nonhydrogen atoms (Fig. 2b), of which 17 atoms belong to the framework and 6 to the guest (DAHP). There are two crystallogrpahically distinct Co atoms and three P atoms. The structure is essentially made up by the vertex linkage of CoO_4 and HPO_4 tetrahedra, forming macroanionic layers. The Co atoms are tetrahedrally coordinated to four oxygen atoms with the Co–O distance in the range 1.922–1.974 Å [$(Co(1)–O)_{av.}$ = 1.953 Å; $(Co(2)–O)_{av.}$ = 1.964 Å] and the O–Co–O angles in the range 97.4°–120.5° [$(O–Co(1)–O)_{av.}$ = 109.5°; $(O–Co(2)–O)_{av.}$ = 109.2°]. The cobalt atoms are connected to three neighboring P atoms via four Co–O–P bonds with an average bond angle of 129.7°. Of the three P atoms, P(1) and P(2) make three P–O–Co bonds and possess one P–O terminal linkage, while P(3) makes two P–O–Co linkages and have two P–O terminal bonds. The

TABLE 7
Selected Bond Distances and Angles in II, $[NH_3CH_2(CH(OH)CH_2NH_3][Co_2(HPO_4)_3]$

Moiety	Distance (Å)	Moiety	Angle (°)
Co(1)–O(1)	1.949(3) [0.4992][a]	O(6)–Co(2)–O(5)	109.87(13)
Co(1)–O(2)	1.969(3) [0.4730]	O(7)–Co(2)–O(8)	115.29(13)
Co(1)–O(3)	1.970(3) [0.4717]	O(6)–Co(2)–O(8)	100.19(13)
Co(1)–O(4)	1.922(3) [0.5370]	O(5)–Co(2)–O(8)	100.67(12)
Co(2)–O(5)	1.963(3) [0.4807]	O(5)–P(1)–O(6)	113.9(2)
Co(2)–O(6)	1.959(3) [0.4859]	$O(5)^{i}$–P(1)–O(2)	111.5(2)
Co(2)–O(7)	1.958(3) [0.4872]	O(6)–P(1)–O(2)	109.1(2)
Co(2)–O(8)	1.974(3) [0.4666]	$O(5)^{i}$–P(1)–O(9)	104.4(2)
P(1)–O(2)	1.519(3) [1.3032]	O(6)–P(1)–O(9)	108.5(2)
P(1)–$O(5)^{i}$	1.516(3) [1.3138]	O(2)–P(1)–O(9)	109.2(2)
P(1)–O(6)	1.517(3) [1.3103]	$O(4)^{ii}$–P(2)–O(8)	111.4(2)
P(1)–O(9)	1.572(3) [1.1293]	$O(4)^{ii}$–P(2)–$O(7)^{iii}$	112.1(2)
P(2)–$O(4)^{ii}$	1.510(3) [1.3353]	O(8)–P(2)–$O(7)^{iii}$	110.4(2)
P(2)–$O(7)^{iii}$	1.529(3) [1.2685]	$O(4)^{ii}$–P(2)–O(10)	108.8(2)
P(2)–O(8)	1.525(3) [1.2822]	O(8)–P(2)–O(10)	105.7(2)
P(2)–O(10)	1.564(3) [1.1540]	$O(7)^{iii}$–P(2)–O(10)	108.2(2)
P(3)–$O(1)^{iv}$	1.509(3) [1.3389]	$O(1)^{iv}$–P(3)–O(12)	110.3(2)
P(3)–O(3)	1.522(3) [1.2927]	$O(1)^{iv}$–P(3)–O(3)	112.5(2)
P(3)–O(11)	1.589(3) [1.0786]	O(12)–P(3)–O(3)	112.5(2)
P(3)–O(12)	1.518(3) [1.3067]	$O(1)^{iv}$–P(3)–O(11)	109.6(2)
Moiety	Angle (°)	O(12)–P(3)–O(11)	104.4(2)
		O(3)–P(3)–O(11)	107.1(2)
O(4)–Co(1)–O(1)	106.6(2)	$P(3)^{iv}$–O(1)–Co(1)	127.3(2)
O(4)–Co(1)–O(2)	110.79(14)	P(1)–O(2)–Co(1)	123.3(2)
O(1)–Co(1)–O(2)	112.51(13)	P(3)–O(3)–Co(1)	129.2(2)
O(4)–Co(1)–O(3)	117.02(14)	$P(2)^{v}$–O(4)–Co(1)	144.8(2)
O(1)–Co(1)–O(3)	112.54(14)	$P(1)^{i}$–O(5)–Co(2)	137.1(2)
O(2)–Co(1)–O(3)	97.35(13)	P(1)–O(6)–Co(2)	125.4(2)
O(7)–Co(2)–O(6)	108.36(13)	$P(2)^{iii}$–O(7)–Co(2)	126.7(2)
O(7)–Co(2)–O(5)	120.49(13)	P(2)–O(8)–Co(2)	124.0(2)

Organic moiety

Moiety	Distance (Å)	Moiety	Angle (°)
N(1)–C(1)	1.483(6)	N(1)–C(1)–C(2)	110.7(4)
C(1)–C(2)	1.517(6)	O(20)–C(2)–C(3)	112.6(4)
C(2)–O(20)	1.407(5)	O(20)–C(2)–C(1)	112.4(4)
C(2)–C(3)	1.509(6)	C(3)–C(2)–C(1)	109.7(4)
C(3)–N(2)	1.484(6)	N(2)–C(3)–C(2)	110.1(4)

Note. Symmetry transformations used to generate equivalent atoms: (i) $-x, -y+1, z+2$; (ii) $x-1, y, z$; (iii) $-x-1, -y+1, -z+2$; (iv) $-x+1, -y, -z+2$; (v) $x+1, y, z$.

[a] Bond valence values are given in brackets.

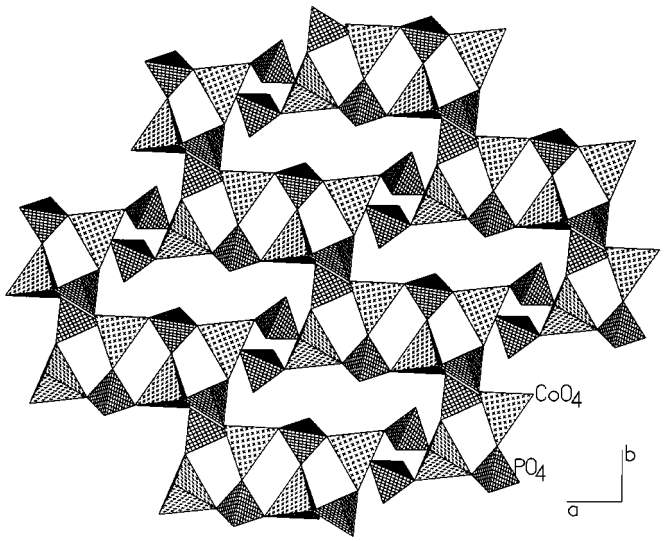

FIG. 5. Structure of **II**, $[NH_3CH_2(CH(OH)CH_2NH_3][Co_2(HPO_4)_3]$, along the *ab* plane showing the connectivity between the CoO_4 and PO_4 tetrahedra within the layer.

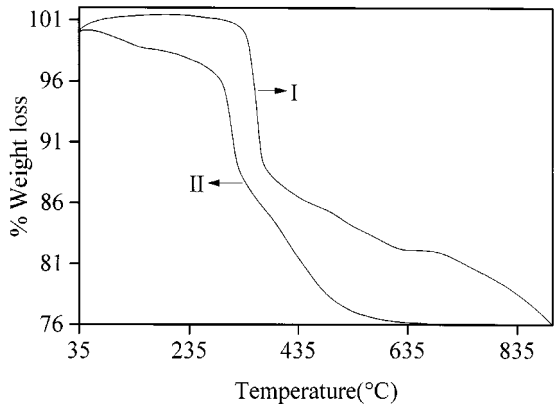

FIG. 7. TGA curve for **I** and **II** showing the weight loss. Note the sharp mass loss around 300°C.

three P atoms have P–O distances in the range 1.510–1.589 Å [$(P(1)–O)_{av.} = 1.531$ Å; $(P(2)–O)_{av.} = 1.532$ Å; $(P(3)–O)_{av.} = 1.535$ Å] and the O–P–O angles are in the range 104.4°–112.5° [$(O–P–O)_{av.} = 109.4°$ for all the P

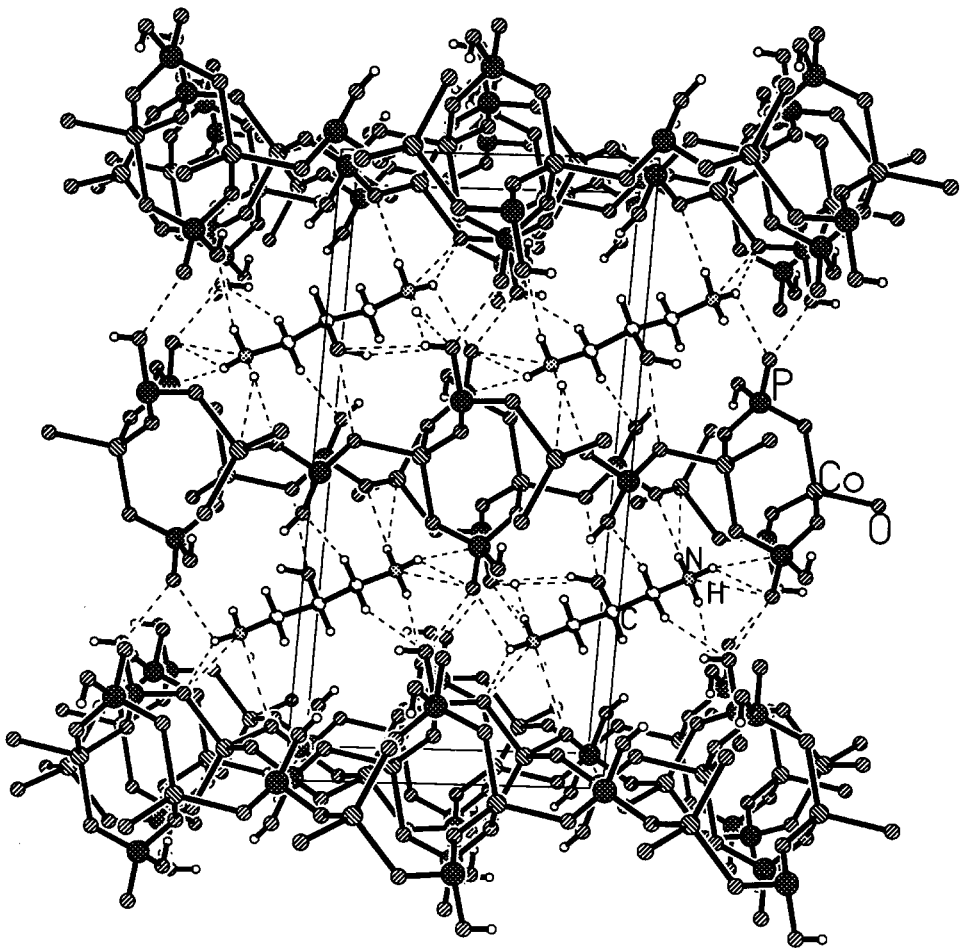

FIG. 6. Structure of **II**, along the *b* axis showing the layer arrangement. The dotted lines represent the hydrogen bond interactions. Note that the amine molecule occupy the pseudo-channels formed by the interframework hydrogen bond interactions.

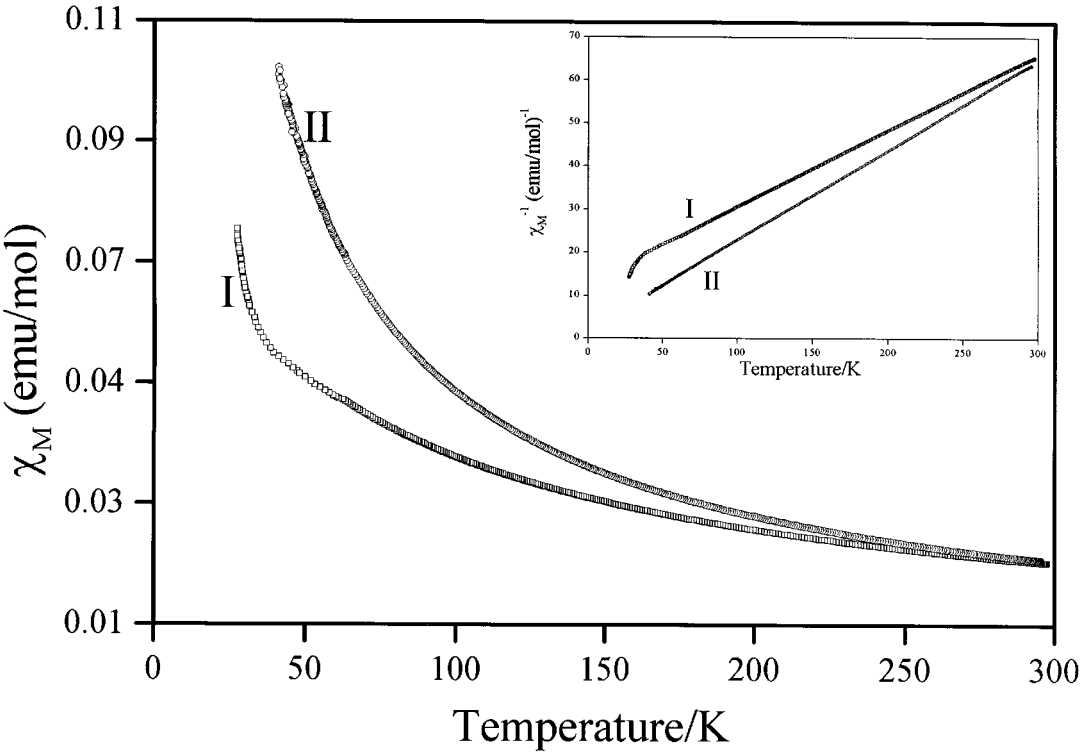

FIG. 8. Magnetic susceptibility data of **I** and **II**. Inverse susceptibility data are shown in the inset.

atoms]. Important bond distances, bond valence parameters, and angles are listed in Table 7. The geometrical parameters observed in **II** are in good agreement with those reported for similar compounds (6–8). Assuming the valences of Co, P, and O to be + 2, + 5, and − 2 respectively, the framework stoichiometry of $Co_2(PO_4)_3$ creates a net framework charge of − 5. Taking into account the presence of doubly protonated DAHP, $[NH_3CH_2\ CH(OH)CH_2NH_3]$, the excess negative charge of − 3 can be balanced by the protonation of the PO_4 tetrahedra. One hydrogen position for each of the oxygens O(9), O(10), and O(12) has been observed in the difference Fourier maps. Thus, P(1)–O(9), P(2)–O(10), and P(3)–O(11) with distances of 1.572, 1.564, and 1.589 Å correspond to P–OH units. The second terminal P–O linkage in the case of P(3) with a P–O distance of 1.518 Å is a P=O unit. These assignments are consistent with bond valence sum calculations (18).

The connectivity between CoO_4 and HPO_4 tetrahedra result in a layered topology based on a two-dimensional network of bifurcated 12-membered rings as shown in Fig. 5. The 12-membered rings consist of 12-T atoms (T = tetrahedra center, Co or P) formed by 6 Co and 6 P atoms which strictly alternate. The layers can be considered to be formed from short chains of 4-membered rings ($Co_2P_2O_4$ units) connected to each other *via* two PO_4 units, creating a bifurcation within the layer. The amine forms the adjacent layer and sits in the middle of this aperture, interacting with the framework via N–H ... O and O–H ... O hydrogen bonding (Fig. 6). The layers in **II** are so formed that the cationic and the anionic layers alternate. The inorganic and organic layers are stacked in the ABABAB fashion just as in one of the open-framework zinc phosphates described recently (19).

TGA for **I** and **II** was carried out under a nitrogen atmosphere in the range room temperature to 700°C, and the results are presented in Fig. 7. Both **I** and **II** show similar behavior with sharp mass losses around 300 and 400°C respectively. The mass loss of ~24% in both cases corresponds well with the loss of the amine. The calcined sample is poorly crystalline (powder XRD) with the majority of lines corresponding to the condensed cobalt phosphate, $Co_2P_2O_7$ [JCPDS: 39-0709].

Magnetic susceptibility data of **I** and **II** are shown in Fig. 8. In the inset of Fig. 8, we show the inverse susceptibility data. What is striking about the data is the behavior of **I** with Co–O–Co chains, becoming ferrimagnetic around 30 K. Compound **II** on the other hand remains paramagnetic. This ferrimagnetic layered cobalt phosphate is similar to that reported by DeBord *et al.* (9). The effective magnetic moments in **I** and **II** are 4.8 and 4.4 μ_B respectively, showing the presence of tetrahedral cobalt in the 2 + oxidation state.

CONCLUSIONS

Two layered cobalt phosphates, **I**, $[NH_3CH_2CH(OH)CH_2NH_3][Co_2(PO_4)_2]$, and **II**, $[NH_3CH_2(CH(OH)CH_2NH_3][Co_2(HPO_4)_3]$, have been synthesized hydrothermally employing the reaction between the amine phosphate (DAHP-P) and Co^{II} ions. The formation of the different cobalt phosphates from the same amine phosphate demonstrates the simultaneous occurrences of different kinetically controlled concentration-dependent processes. Although both **I** and **II** have layered architecture, **I** possesses 3- and 4-membered apertures while **II** has 4- and 12-membered apertures within the layers. Both structures are stabilized by extensive hydrogen bond interactions involving the hydrogens of the amine molecules and the framework oxygens. The synthesis of two layered cobalt phosphates using the amine phosphate route shows that it should be possible to synthesize new members of cobalt and other transition metal phosphates by a suitable choice of amine phosphates and reaction conditions.

ACKNOWLDGMENTS

A.C. thanks the Council of Scientific and Industrial Research (CSIR), Government of India for the award of a research fellowship.

REFERENCES

1. A. K. Cheetham, T. Loiseau, and G. Ferey, *Angew. Chem. Int. Ed.* **38,** 3268 (1999).
2. (a) M. Cavellec, D. Riou, and G. Ferey, *J. Solid State Chem.* **112,** 441 (1994); (b) M. Cavellec, D. Riou, J.-M. Greneche, and G. Ferey, *Zeolites* **17,** 252 (1996); (c) M. Cavellec, C. Egger, J. Linares, M. Nogues, F. Varret, and G. Ferey, *J. Solid State Chem.* **134,** 349 (1997); (d) M. R. Cavellec, J.-M. Greneche, D. Riou, and G. Ferey, *Chem. Mater.* **10,** 2434 (1998); (e) M. Cavellec, J.-M. Greneche, D. Riou, and G. Ferey, *Microporous Mater.* **8,** 103 (1997); (f) M. Cavellec, D. Riou, J.-M. Greneche, and G. Ferey, *J. Magn. Magn. Mater.* **163,** 173 (1996); (g) M. Cavellec, D. Riou, and G. Ferey, *Acta Crystallogr. Sect. C* **51,** 2242 (1995); (h) M. Riou-Cavellec, J.-M. Greneche, and G. Ferey, *J. Solid State Chem.* **148,** 150 (1999).
3. (a) C.-Y. Huang, S.-L. Wang, and K.-H. Lii, *J. Porous Mater.* **5,** 147 (1998); (b) K.-H. Lii, Y.-F. Huang, V. Zima, C.-Y. Huang, H.-M. Lin, Y.-C. Jiang, F.-L. Liao, and S.-L. Wang, *Chem. Mater.* **10,** 2599 (1998) and references therein: (c) J. R. D. DeBord, W. M. Reiff, C. J. Warren, R. C. Haushalter, and J. Zubieta, *Chem. Mater.* **9,** 1994 (1997); (d) J. R. D. DeBord, W. M. Reiff, R. C. Haushalter, and J. Zubieta, *J. Solid State Chem.* **125,** 186 (1996).
4. (a) A. Mgaidi, H. Boughzala, A. Driss, R. Clerac, and C. Coulon, *J. Solid State Chem.* **144,** 163 (1999); (b) Z. A. D. Lethbridge, P. Lightfoot, R. E. Morris, D. S. Wragg, P. A. Wright, Å. Kvick, and G. Vaughan, *J. Solid State Chem.* **142,** 455 (1999).
5. (a) A. Choudhury and S. Natarajan, *Proc. Ind. Natl. Acad.* (*Chem. Sci.*) **111,** 627 (1999); (b) A. Choudhury, S. Natarajan, and C. N. R. Rao, *Chem. Commun.* 1305 (1999); (c) A. Choudhury and S. Natarajan, *Int. J. Inorg. Mater.* **2,** 217 (2000).
6. J. Chen, R. H. Jones, S. Natarajan, M. B. Hursthouse, and J. M. Thomas, *Angew. Chem. Int. Ed. Engl.* **33,** 639 (1994).
7. (a) P. Feng, X. Bu, S. H. Tolbert, and G. D. Stucky, *J. Am. Chem. Soc.* **119,** 2497 (1997); (b) P. Feng, X. Bu, and G. D. Stucky, *J. Solid State Chem.* **129,** 328 (1997); (c) P. Feng, X. Bu, and G. D. Stucky, *J. Solid State Chem.* **131,** 160 (1997); (d) P. Feng, X. Bu, and G. D. Stucky, *J. Solid State Chem.* **131,** 387 (1997).
8. (a) X. Bu, P. Feng, T. E. Gier, and G. D. Stucky, *J. Solid State Chem.* **136,** 210 (1998); (b) P. Feng, X. Bu, and G. D. Stucky, *Nature* **388,** 735 (1997); (c) X. Bu, P. Feng, and G. D. Stucky, *Science* **278,** 2080 (1997).
9. J. R. D. DeBord, R. C. Haushalter, and J. Zubieta, *J. Solid State Chem.* **125,** 270 (1996).
10. S. Neeraj, S. Natarajan, and C. N. R. Rao, *Angew. Chem. Int. Ed.* **38,** 3480 (1999).
11. C. N. R. Rao, S. Natarajan, and S. Neeraj, *J. Am. Chem. Soc.* **122,** 2810 (2000).
12. (a) S. Natarajan, S. Neeraj, A. Choudhury, and C. N. R. Rao, *Inorg. Chem.* **39,** 1426 (2000); (b) S. Natarajan, S. Neeraj, and C. N. R. Rao, *Solid State Sci.* **2,** 89 (2000).
13. "Siemens Users Manual," Siemens Analytical X-ray Instruments, Madison, WI, 1995.
14. G. M. Sheldrick, "SADABS Siemens Area Detector Absorption Correction Program," University of Gottingen, Gottingen, Germany, 1994.
15. G. M. Sheldrick, "SHELXS-86, A Program for the Solution of Crystal Structures," University of Göttingen, Göttingen, Germany, 1986.
16. G. M. Sheldrick, "SHELXTL-PLUS Program for Crystal Structure Solution and Refinement," University of Göttingen, Göttingen, Germany, 1993.
17. C. N. R. Rao, S. Natarajan, and S. Neeraj, *J. Solid State Chem.* **152,** 302 (2000).
18. I. D. Brown and D. Aldermatt, *Acta Crystallogr. Sect. B* **41,** 244 (1984).
19. D. Chidambaram, S. Neeraj, S. Natarajan, and C. N. R. Rao, *J. Solid State Chem.* **147,** 154 (1999).